Forschungszentrum Karlsruhe
in der Helmholtz-Gemeinschaft

Wissenschaftliche Berichte
FZKA 7069

Magnetohydrodynamic Flow in the European HCLL Blanket Concept

L. Bühler, L. Giancarli

Institut für Kern- und Energietechnik
Programm Kernfusion

Mai 2005

Forschungszentrum Karlsruhe

in der Helmholtz-Gemeinschaft

Wissenschaftliche Berichte

FZKA 7069

Magnetohydrodynamic flow in the European HCLL blanket concept

L. Bühler and L. Giancarli [*]

Institut für Kern- und Energietechnik
Programm Kernfusion

[*]CEA, Saclay, France

Forschungszentrum Karlsruhe GmbH, Karlsruhe
2005

Impressum der Print-Ausgabe:

Als Manuskript gedruckt

Forschungszentrum Karlsruhe GmbH
Postfach 3640, 76021 Karlsruhe

Mitglied der Hermann von Helmholtz-Gemeinschaft
Deutscher Forschungszentren (HGF)

ISSN 0947-8620

urn:nbn:de:0005-070692

Magnetohydrodynamic flow in the European HCLL blanket

Abstract

Magnetohydrodynamic flows in a helium cooled lead lithium blanket for a future power reactor is analyzed by combined asymptotic- numeric computations. The flow is considered in real 3D geometries given by the design. The global geometry is decomposed into main geometric elements. Of special concern are the connections between the circular access tubes with the breeder boxes through poloidal manifolds. The flow then enters the breeder box through narrow distributing gaps. Another important geometric element is the region near the first wall, where the fluid has to pass another narrow gap. For applications to a power reactor, pressure drops of the order of $\Delta p^* = 0.27\,\mathrm{MPa}$ have been estimated for an applied magnetic field of $B = 5\,\mathrm{T}$. It turns out that the major fraction of this pressure drop arises in the poloidal manifold. For that reason further improvements in the design should focus on this particular detail.

Magnetohydrodynamische Strömungen im Europäischen HCLL Blanket

Zusammenfassung

Mit einer kombinierten asymptotisch - numerischen Analyse werden magnetohydrodynamische Strömungen in einem Helium-gekühlten Blei-Lithium- Blanket eines zukünftigen Fusionsreaktors untersucht. Die Strömung wird in realistischen 3D Geometrien untersucht, die durch das Design des Blankets vorgegeben sind. Die Gesamtgeometrie wird hierzu in typische geometrische Elemente zerlegt. Besonderes Interesse gilt den Verbindungen zwischen den kreisförmigen Zuleitungen und den Brütereinheiten über poloidale Verteiler. Dabei tritt die Strömung durch einen engen Spalt in die Bruteinheit ein. Ein weiteres wichtiges geometrisches Element befindet sich nahe der ersten Wand, wo das Fluid ebenfalls einen engen Spalt überwinden muss. Eine Abschätzung für Anwendungen in einem Leistungsreaktor ergibt Druckverluste von der Größenordnung $\Delta p^* = 0.27\,\mathrm{MPa}$ in einem Magnetfeld von $B = 5\,\mathrm{T}$. Es zeigt sich, dass der Hauptanteil dieses Druckverlusts im poloidalen Verteiler entsteht. Weitere Verbesserungen im Design sollten sich deshalb auf dieses spezielle Detail konzentrieren.

Magnetohydrodynamic flow in the European HCLL blanket

Contents

1 Introduction

Liquid metal magnetohydrodynamic (MHD) flows in a helium cooled lithium lead (HCLL) blanket for a future power reactor are investigated. In this type of blanket the liquid metal lithium lead serves exclusively as breeder material. The total heat is extracted by a number of gas-cooled plates through which the coolant helium is circulated at high speed and high pressure. The liquid metal is located in gaps between these cooling plates and convection is not required for heat removal. Nevertheless, a weak liquid metal circulation is foreseen for purification of the breeder and tritium extraction.

The liquid metal is supplied through a relatively small circular pipe into a poloidal manifold from which it enters the much larger breeder boxes through narrow gaps. A global sketch of the geometry is shown in Fig. 1. The breeder unit with the distributing gap is shown in Fig. 2. A sketch of the poloidal manifold is shown in Fig. 3. The connection of this manifold with the breeder units is shown in Fig. 4.

Since in the current design feeding pipes and poloidal manifolds are relatively small compared with the dimensions of the breeding boxes the velocities there may reach such values that the major fraction of the pressure drop arises rather in these ducts than in the breeder boxes. In the actual design for a power reactor one poloidal manifold supplies a number of 8 breeder units. These are connected at the first wall with other 8 units. The latter ones are drained at the back plate through a circular tube similarly to the entrance geometry. A more detailed description of the design is given by Rampal, Poitevin, Li-Puma, Rigal, Szczepanski and Boudot (2004).

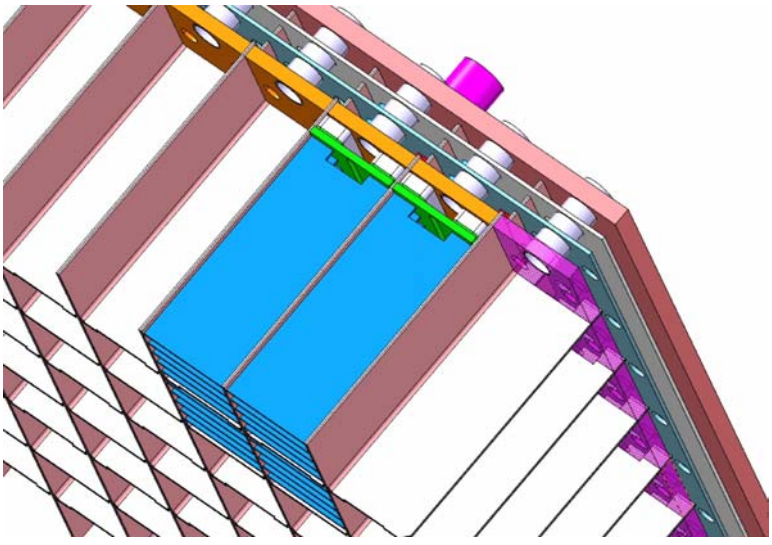

Figure 1: View of an entire HCLL module. One can see the liquid metal circular access tubes (white), the poloidal manifold, distributing gap (entrance into the breeder unit through green plate) and the cooling plates (blue).

For practical reasons, the total geometry with all breeder units is decomposed into characteristic elements for which a numerical analysis is performed. It is possible to identify typical values of pressure drop for individual geometric elements. On that basis

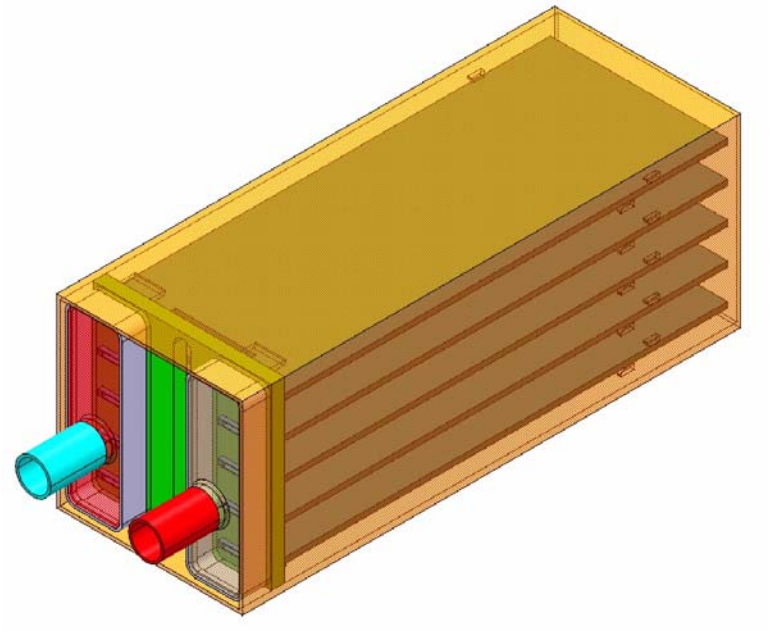

Figure 2: View on a breeder unit. The liquid metal enters the unit through a narrow gap in the rear (green) plate. Later it flows in gaps between the 5 cooling plates.

the overall performance is estimated by combining each contribution to the total pressure drop.

The flow path can be summarized in a principle flow scheme as shown in Fig. 5. The flow enters the module through a single access tube, passes the poloidal manifold and enters into 8 breeder units. At the first wall there is a connection with other 8 units, then the flow is collected in a second poloidal manifold before it leaves the module through a single pipe.

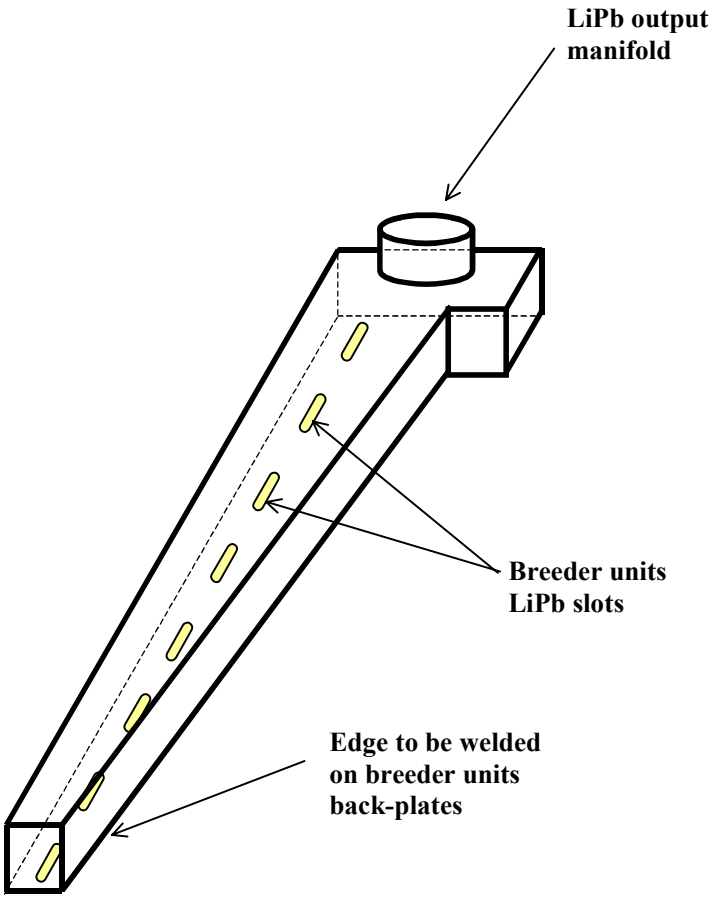

Figure 3: One part of the poloidal manifold. Device used to separate LiPb input from output flow in PPCS modules (16 breeding units per column)

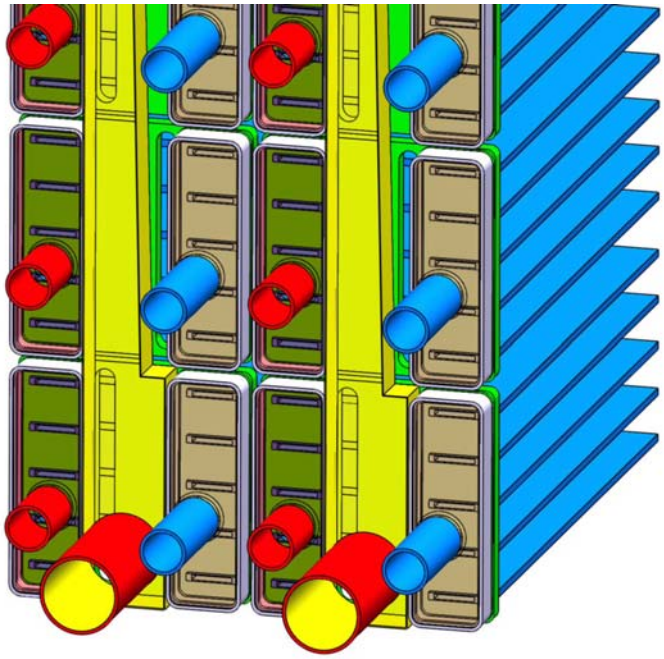

Figure 4: View on the poloidal manifold (yellow) and breeder units.

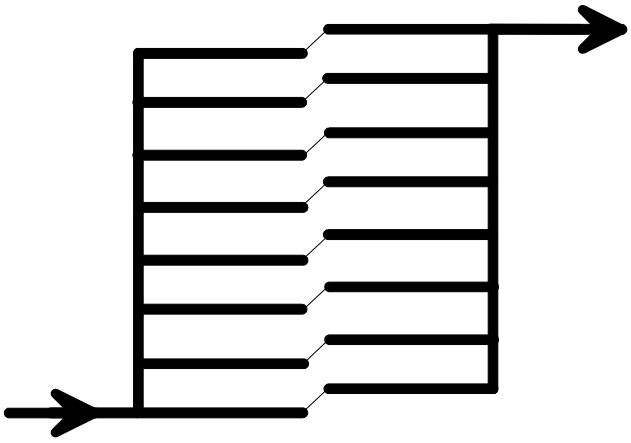

Figure 5: Principle flow scheme through a HCLL blanket of a power reactor.

2 Formulation

The inertialess, inductionless magnetohydrodynamic flow in a HCLL blanket of a power reactor is governed by the balance of momentum

$$\nabla p = \frac{1}{Ha^2}\nabla^2 \mathbf{v} + \mathbf{j} \times \mathbf{B}, \tag{1}$$

conservation of mass

$$\nabla \cdot \mathbf{v} = 0 \tag{2}$$

and charge

$$\nabla \cdot \mathbf{j} = 0, \tag{3}$$

and by Ohm's law

$$\mathbf{j} = -\nabla\phi + \mathbf{v} \times \mathbf{B}. \tag{4}$$

In the equations shown above, $\mathbf{v}$, $\mathbf{B}$, $\mathbf{j}$, p, ϕ stand for velocity, magnetic induction, current density, pressure and electric potential, scaled by the reference quantities v_0, B_0, $j_0 = \sigma v_0 B_0$, $p_0 = \sigma v_0 B_0^2 L$ and $\phi_0 = v_0 B_0 L$, respectively. The scale of velocity v_0 is the average velocity in the circular access tube (for feeding one breeder unit) and L is the radius of that tube. The quantity B_0 is the magnitude of the applied magnetic induction. For this first assessment of pressure drop B_0 is assumed to be uniform. The electric conductivity σ, the kinematic viscosity ν, and the density ρ are assumed to be constant. Material properties for the fluid are taken from Jauch, Karcher, Schulz and Haase (1986) and for walls from Tavassoli (2002).

The inertialess assumption is usually justified for high interaction parameters $N \gg 1$ so that the flow considered here is governed uniquely by the Hartmann number Ha. These quantities are defined as

$$\begin{aligned} Ha &= B_0 L \sqrt{\frac{\sigma}{\rho\nu}}\,, \\ N &= \frac{\sigma L B_0^2}{\rho v_0}\,. \end{aligned}$$

The square of the Hartmann number characterizes the ratio of electromagnetic forces to viscous forces while the interaction parameter represents the ratio of electromagnetic forces to inertia forces. For the current design we have typically

$$Ha \gtrsim 10^4 \tag{5}$$

and often

$$N \gtrsim 10^4. \tag{6}$$

At the fluid wall interface there is no-slip,

$$\mathbf{v} = 0, \tag{7}$$

and continuity of electric potential

$$\phi = \phi_w. \tag{8}$$

The wall potential ϕ_w is obtained from the thin wall condition (Walker (1981))

$$\mathbf{j} \cdot \mathbf{n} = \nabla \cdot (c \nabla_t \phi_w) \,. \tag{9}$$

Here ∇_t denotes the components of the gradient operator in plane tangential to the wall. The wall conductance ratio

$$c = \frac{\sigma_w t_w}{\sigma L} \tag{10}$$

describes the electric conductivity of the wall with thickness t_w compared with the conductivity of the fluid. Internal helium channels are taken into account by a reduced effective conductivity according to the "porosity" of the wall.

The inertialess flow outside the viscous layers is calculated using a numerical code based on asymptotic techniques that is able to solve the MHD equations in almost arbitrary domains. The code applies best for cases where $N \rightarrow \infty$ and $Ha \gg 1$. Moreover, the flow in the core becomes independent of Ha if the wall conductance c is much higher than the conductivity of the viscous boundary layers located at that wall. This is the case in the present problem. If details of the flow in the layers are required it is straight forward to evaluate any information needed once the solution in the core is known. The code uses a boundary fitted coordinate system that allows for an efficient modelling of complicated 3D geometries. A detailed description of the code and a number of application examples has been published by Bühler (1995).

3 Manifold into a single breeder unit

We consider in this section a MHD flow through a circular feeding pipe into a first cubic manifold of larger dimension, i.e. the poloidal manifold. From the manifold reservoir the flow is distributed into the breeder box through a narrow gap. It is assumed that the magnetic field is uniform over the entire computational domain. The requirement that the breeder should be exchanged ten times a day results in velocities through the access tube of $v_0 = 2.4\,\mathrm{mm\,/\,s}$ (W. Farabolini, private communication 2004) for feeding one breeder unit. Since one tube feeds a number of 8 breeder units for a power reactor, the velocity in the access tube reaches values of $8v_0$, respectively. For a lack of computational resources it is not possible to study the entire assembly of all breeder units. Therefore we focus the analysis on one unit as shown in Fig. 8 and draw later conclusions that extrapolate our knowledge to the entire present design. For simplicity the internal cooling plates in the breeder boxes have been removed for this first assessment. The present geometry represents just one essential detail of the global flow path as shown in Fig. 6 (indicated by blue circles).

The numerical calculations are performed using a non - equidistant grid as shown in Fig. 7. This grid concentrates a large number of points near the 3D regions.

The surface in Fig. 8 is colored by electric potential contours. In the feeding pipe we observe highest transverse potential gradients created by the flow which has the highest speed in this region. Along its path the cross section becomes bigger, the velocities become smaller and therefore the potential observed on the surface decreases. The only region where the velocity increases again is the narrow connection between the breeder unit and the manifold. However, the large volumes of fluid at both sides of the constriction allow for an immediate shortcut of currents so that finally the values of potential remain relatively modest in these regions.

Most important is the knowledge about MHD pressure drop in such geometries. In order to get an immediate impression we look at the distribution of pressure along the top and bottom of the geometry at $z_{\max}$ and $z_{\min}$ and along the center of each cross section. Results are displayed in Fig. 9. At the entrance of the circular pipe and at

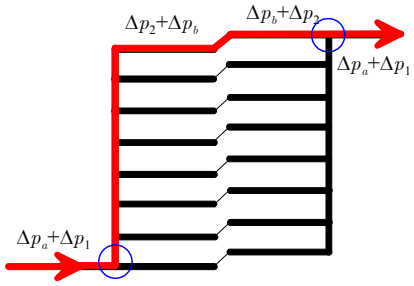

Figure 6: Flow scheme showing a single flow path in red. The focus in this section is on the details indicated by blue circles and on the individual pressure drop contributions shown in the figure.

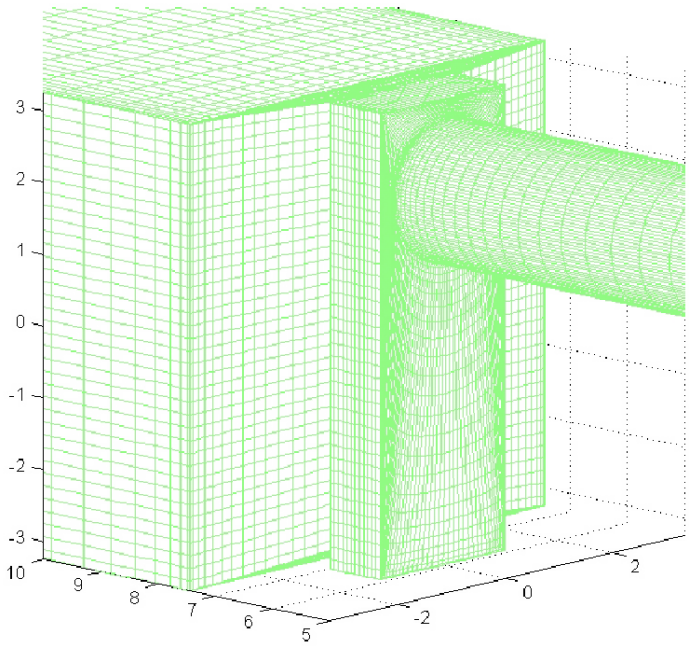

Figure 7: Details of the surface grid near the manifold.

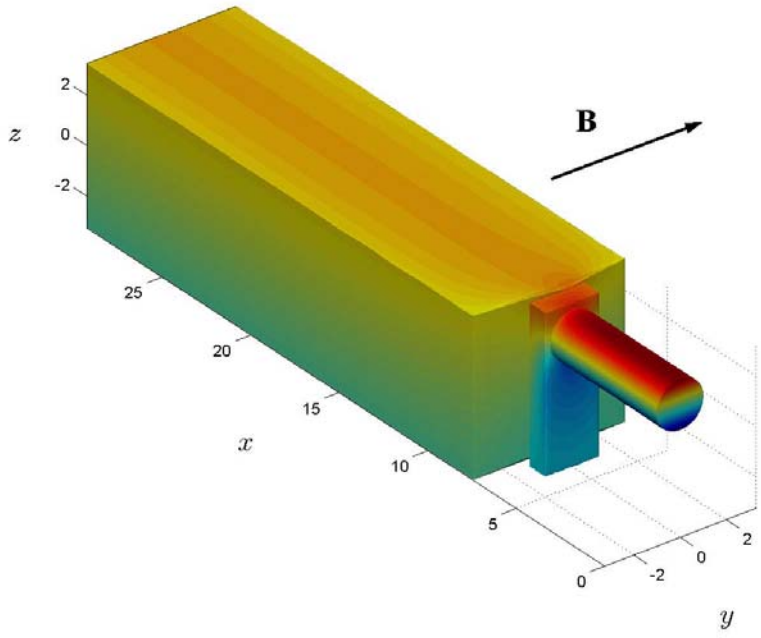

Figure 8: Colored contours of electric potential on the surface of the geometry

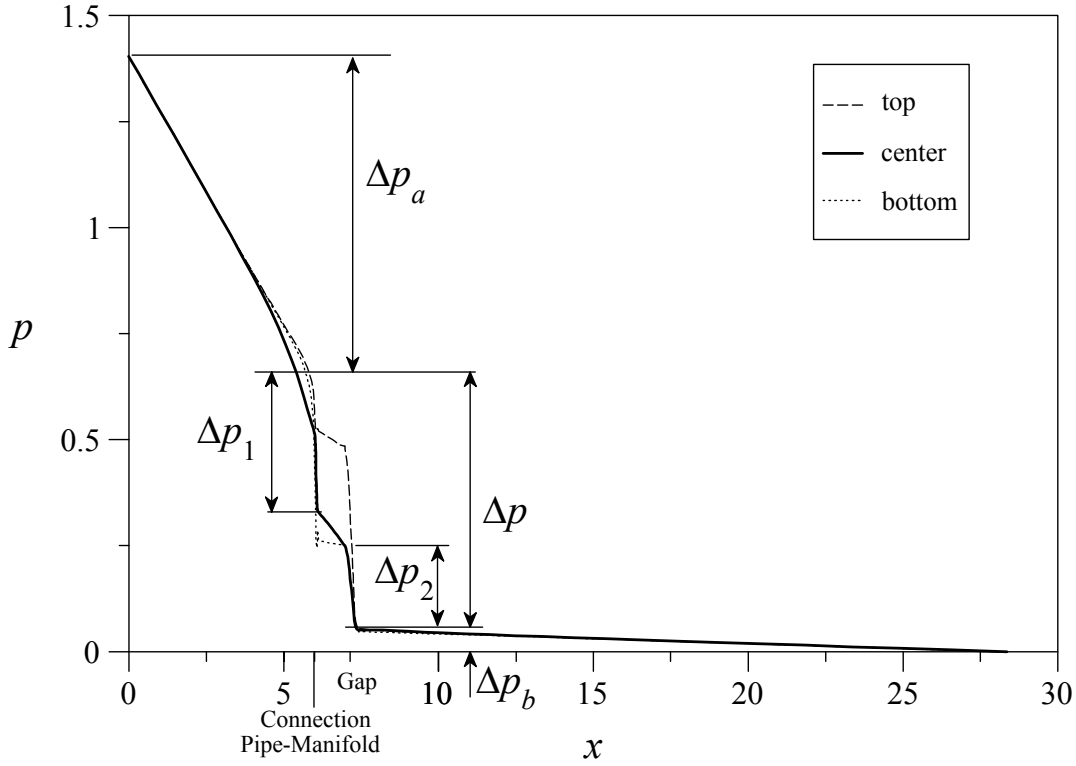

Figure 9: Pressure along the flow path through the manifold distributing gap, and along breeder unit.

the exit of the rectangular duct we observe fully established flow regimes characterized by uniform pressure gradients. Through the access tube the non-dimensional pressure drops by $\Delta p_a \approx 0.74$. The pressure drop $\Delta p_b \approx 0.06$ accounts for the pressure drop of the breeder unit, a value that is fairly small compared with the other pressure losses. We observe in this figure two regions in which the pressure drops very rapidly. One is at the place where the circular pipe is connected to the manifold and the other is located at the gap which connects the manifold with the breeder unit. The connecting gap acts similar as a nozzle and equilibrates pressure in the whole cross section. If we consider the variation of pressure along the center of cross sections we may distinguish between the two main contributions $\Delta p_1 \approx 0.33$ and $\Delta p_2 \approx 0.19$ that occur at the circular- to rectangular connection and at the distributing gap connecting the manifold with the breeder box, respectively.

The splitting between these different pressure drops is reasonable since one circular pipe has to feed a number of breeder units giving rise to several times the value of $(\Delta p_a + \Delta p_1)$, while $\Delta p_2 + \Delta p_b$ occurs only once for each individual breeder unit (see Sect. 5). The numerical values are for pressure drop are summarized as

$$\begin{aligned} \Delta p_a &\approx 0.74, \qquad \Delta p_1 \approx 0.33, \\ \Delta p_2 &\approx 0.19, \qquad \Delta p_b \approx 0.06. \end{aligned} \tag{11}$$

4 Connection of two breeder units

The other important 3D geometry is located near the first wall, where two breeder boxes are connected through a narrow gap at the common dividing wall. For the position of this 3D element in the global flow scheme see Fig. 10. The real geometry is displayed in Fig 11. This geometry forms basically a bend in the plane perpendicular to the magnetic field, i.e. in a radial-poloidal plane. It is especially the (20%) reduction of length measured along **B** that causes the additional pressure drop. We observe a potential difference between the side walls of the bend (the inner and the outer walls) which does not vary too much along the flow path.

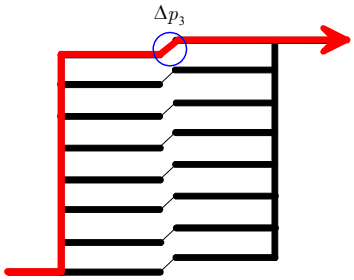

Figure 10: Flow scheme showing a single flow path colored in red. The focus in this section is on the detail indicated by blue circle and on the individual pressure drop contribution Δp_3.

For engineering purposes the variation of the non-dimensional pressure along the inner and outer wall is plotted over the axial position as well as the pressure in the center of the cross section. From Fig. 12 we conclude that the extra pressure drop reaches values of approximately $\Delta p_3 = 0.038$. Nevertheless, this value is fairly small compared with the pressure drop created in the manifold.

For thin walls isolines of electric potential may be interpreted as approximate streamlines for the fluid flow (see e.g. Müller and Bühler (2001)). Figure 11 indicates therefore, that without internal cooling plates the flow starts to turn in the direction of the slot already at a distance of $5L$ from the first wall. With internal cooling plates the flow has to follow the radial direction over a longer distance. This additional constraint could affect the flow in the sense that the total pressure drop increases further in comparison with the flow in the breeder unit with removed cooling plates. This topic, however, is out of scope of the present work and will be considered in future. On the other hand, estimates for total pressure drop show that the contribution due to the flow in the breeder box contributes only weakly so that further details here will not significantly influence the global behavior.

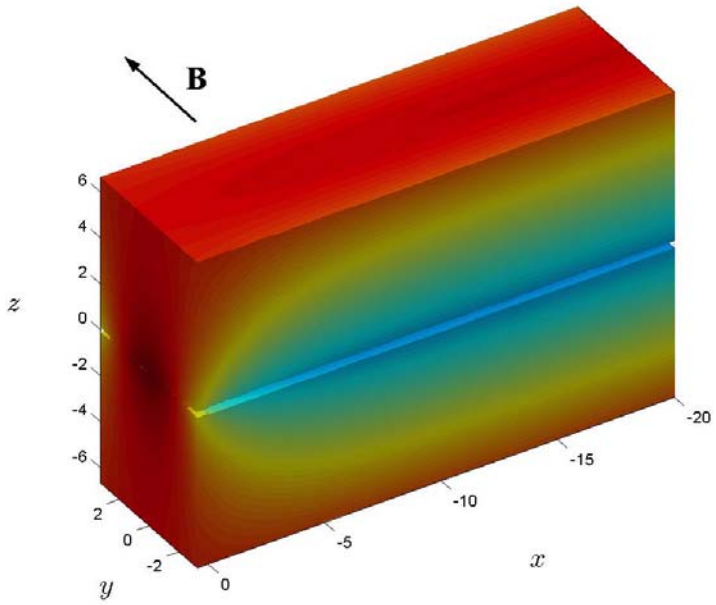

Figure 11: Electric potential on the surface of two breeder units near their connection at the first wall.

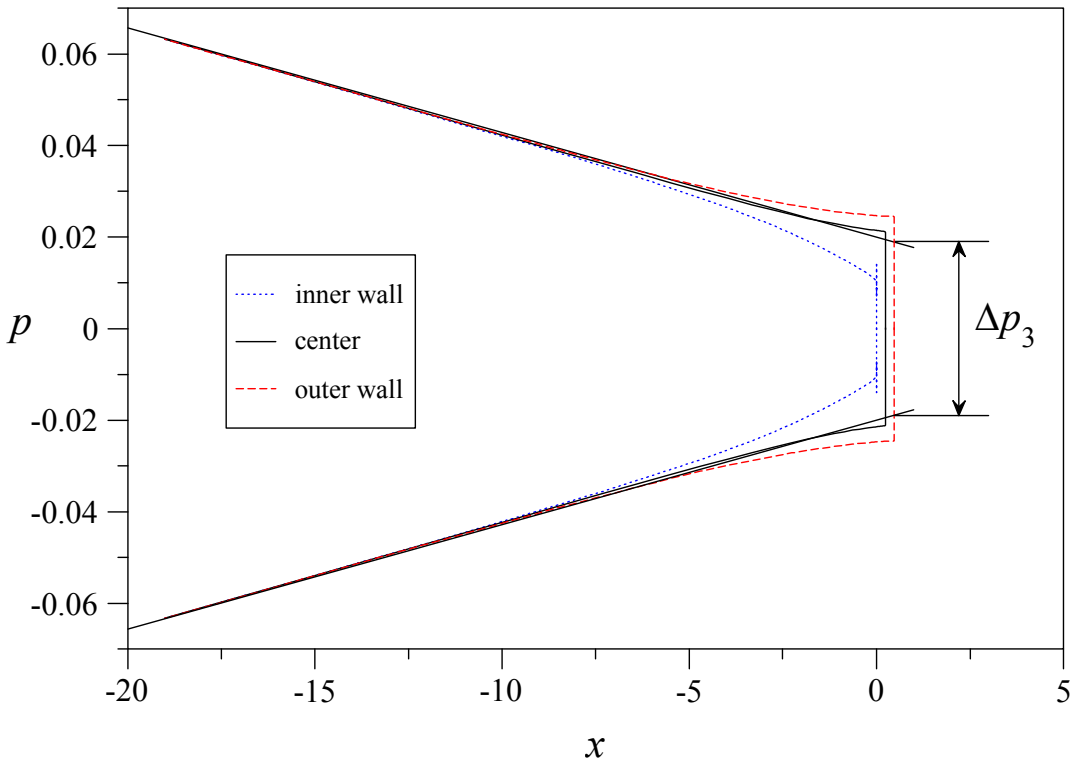

Figure 12: Pressure along the outer and inner surface and in the center of the two breeder units near the first wall.

5 Estimation of total pressure drop

For a power reactor the total number of breeder units arranged in a column is 16. The half of them is fed by the poloidal manifold, while the other half is drained by the poloidal manifold. The total pressure drop of the whole assembly is estimated in the following based on the details obtained above. A flow scheme of the whole assembly is shown in Fig.13. The total pressure drop is immediately estimated from that figure as

$$\Delta p_{tot} = 16\,(\Delta p_a + \Delta p_1) + 2\,(\Delta p_2 + \Delta p_b) + \Delta p_3 + 8\Delta p_m. \tag{12}$$

The factors of 8 or 16 in the formula (12) arises from the fact that one feeding pipe has to supply 8 breeder units. This gives 8 times higher velocity in these regions than was used in our calculations. As a consequence we expect 8 times higher pressure drop, both, at the entrance and at the exit but also along the poloidal manifold.

The variable Δp_m stands here for the pressure drop in the long poloidal manifold. For simplicity we assume the flow in the manifold as a purely poloidal duct flow in a cross section of nondimensional scale 2.17×0.875 along a poloidal length of $l_m = 101.2$. The flow rate in this duct for feeding one breeder unit is the same as that passing through the circular access tube, i.e. $\int u\,da = \pi$. This leads to the results that the average velocity here is $1.6\,v_0$. Using a conductivity of the wall as $c = 0.194$ (4 mm thick solid EUROFER) as Hartmann walls and $c = 0.73$ (15 mm thick solid EUROFER back plates) as side walls we find $\Delta p_m = 21.6$. The poloidal manifold feeds 8 BUs so that this contribution occurs 8 times in (12).

In summary we find

$$\Delta p_{tot} = 191 \tag{13}$$

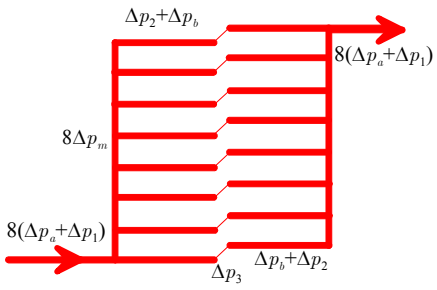

Figure 13: Sketch for assembling of results for pressure drop.

In order to give design relevant data we return to a dimensional representation. The pressure drop is obtained generally by rescaling as

$$\Delta p^* = \Delta p_{tot}\; p_0, \tag{14}$$

where the reference pressure difference according to the section *Formulation* is

$$p_0 = \sigma v_0 B^2 L. \tag{15}$$

For the current geometry, and $\sigma = 0.75 \cdot 10^6\,(\Omega\,\mathrm{m})^{-1}$, $v_0 = 2.4\,\mathrm{mm\,/\,s}$, $L = 32\,\mathrm{mm}$, we find values of

$$\begin{aligned} \Delta p^* &= 0.27\,\mathrm{MPa} \quad \text{for} \quad B = 5\,\mathrm{T}, \\ \Delta p^* &= 1.1\,\mathrm{MPa} \quad \text{for} \quad B = 10\,\mathrm{T}\,. \end{aligned} \tag{16}$$

This result is just an example for a typical magnitude of a magnetic field. The latter formula (14) is flexible enough to account easily for different velocities, or for different magnetic fields as they appear at different poloidal positions.

The pressure drop estimated so far is based on the assumption of inertialess flow conditions. This assumption is fairly justified for the flow in the breeder units. At the 3D elements near the access tubes the velocities are higher, so that inertia may give some additional contributions to the pressure drop. Nevertheless, since the interaction parameter is still high, it is expected that these contributions remain small in comparison with the total pressure drop. For this first assessment the cooling plates in the breeder units have been removed. With cooling plates inserted, the velocity in the breeder units is larger and therefore the pressure drop expected there will be higher. However, since the pressure drop in the breeder units gives only a minor contribution to the total pressure drop it is expected that the overall performance of the blanket will not change significantly by the presence of cooling plates.

6 Conclusions

The MHD flow in main components of a HCLL blanket has been analyzed for a power reactor. Those components are the circular feeding pipe, the poloidal manifold, the breeder box and the flow through the gap at the first wall. As an example only a single box with its connection has been studied by detailed numerical modelling. Different individual contributions to the total pressure drop have been identified and the total pressure drop for a power reactor blanket module has been estimated by reasonable extrapolation. As a result from the current work we find that the pressure drop in the breeder boxes is very small compared with the pressure drop in the piping system supplying the boxes with liquid metal. The major pressure drop arises in the poloidal manifold that connects a number of breeder units. For 16 breeder units in a column we estimate a total pressure drop of about $\Delta p^* = 0.27\,\mathrm{MPa}$ for a magnetic field of $B = 5\,\mathrm{T}$ or , $\Delta p^* = 1.1\,\mathrm{MPa}$ for $B = 10\,\mathrm{T}$. Such values seem acceptable for the current reactor design. Nevertheless it is worth to think about further improvement of the design in order to minimize MHD pressure losses.

The results described in this report are based on latest design information that was available at the beginning of December 2004. The present results can be modified or extended in future for judging about the global performance of a HCLL blanket, once more details about the geometry of the piping system behind the back plates is known.

References

Bühler, L.: 1995, Magnetohydrodynamic flows in arbitrary geometries in strong, nonuniform magnetic fields, *Fusion Technology* **27**, 3–24.

Jauch, U., Karcher, V., Schulz, B. and Haase, G.: 1986, Thermophysical properties in the system Li-Pb, *Technical Report KfK 4144*, Kernforschungszentrum Karlsruhe.

Müller, U. and Bühler, L.: 2001, *Magnetofluiddynamics in Channels and Containers*, Springer, Wien, New York. ISBN 3-540-41253-0.

Rampal, G., Poitevin, Y., Li-Puma, A., Rigal, E., Szczepanski, J. and Boudot, C.: 2004, HCLL TBM for ITER - design studies, *Fusion Engineering and Design* . Presentation at the 23rd Symposium on Fusion Technology, 20-24 September.

Tavassoli, F.: 2002, DEMO interim structural design criteria. Appendix A Material Design Limit Data A3.S18E EUROFER steel, *Technical Report CEA/DEN/SAC/DMN D0-155-21/06/02*, Commissariat à l'Energie Atomique.

Walker, J. S.: 1981, Magnetohydrodynamic flows in rectangular ducts with thin conducting walls, *Journal de Mécanique* **20**(1), 79–112.